

A flagellar K^+ -dependent Na^+/Ca^{2+} exchanger keeps Ca^{2+} low in sea urchin spermatozoa

Yi-Hsien Su and Victor D. Vacquier*

Center for Marine Biotechnology and Biomedicine, Scripps Institution of Oceanography, University of California at San Diego, La Jolla, CA 92093-0202

Communicated by David L. Garbers, University of Texas Southwestern Medical Center, Dallas, TX, March 29, 2002 (received for review February 14, 2002)

The metabolism, flagellar beating, and acrosome reaction of spermatozoa are regulated by ion flux across the plasma membrane. As is true of most cells, swimming sperm maintain intracellular Ca^{2+} concentrations at submicromolar levels. Here we describe a K^+ -dependent Na^+/Ca^{2+} exchanger (suNCKX) from sea urchin sperm. The suNCKX is phylogenetically related to other NCKXs, which use high relative intracellular K^+ , and high relative extracellular Na^+ , to couple the efflux of 1 Ca^{2+} and 1 K^+ to the influx of 4 Na^+ . The 652-aa suNCKX shares structural topology with other NCKX proteins, and has two protein kinase A sites and a His-rich region in its cytoplasmic loop. The suNCKX is encoded by a single gene, which is highly expressed in testes. The suNCKX activity of whole sperm shows Na^+ and K^+ dependence, and like other NCKXs can run in reverse exchange mode. An inhibitor blocks the suNCKX activity and sperm motility. suNCKX localizes to the plasma membrane over the sperm flagellum. The suNCKX may play a major role in keeping Ca^{2+} low in swimming sperm.

sperm motility | ion exchangers | fertilization | flagellar ion exchange

Cells generally maintain intracellular free Ca^{2+} at submicromolar levels (1). In some cells, Ca^{2+} affects the velocity of sliding and bending of axonemal microtubules (2–4). For marine spermatozoa, the internal Ca^{2+} concentration greatly influences the pattern and shape of flagellar bending. In Triton-demembrated, ATP-reactivated sea urchin sperm, elevated Ca^{2+} increases flagellar beat asymmetry (5, 6) and reversibly blocks beating at 0.1–0.2 mM (7). It has been proposed that these actions are mediated by separate high- and low-affinity “ Ca^{2+} sensors” (8). Intact, swimming sea urchin sperm occasionally stop for ≈ 1 s then reinitiate motility. This periodic quiescence requires 2 mM external Ca^{2+} . Increasing K^+ in the medium to 80 mM increases the proportion of quiescent cells (9). The mechanism by which swimming sperm maintain low intracellular Ca^{2+} is not known (10).

Plasma membrane Na^+/Ca^{2+} exchangers are one way in which cells regulate Ca^{2+} (11). These exchangers divide into two major families: Na^+/Ca^{2+} exchangers (NCX) and K^+ -dependent Na^+/Ca^{2+} exchangers (NCKX). Both types of exchangers can run in either direction; however, they usually couple high external Na^+ (NCX type), or high external Na^+ and high internal K^+ (NCKX type), to transport Ca^{2+} out of the cell. There are three known NCX subfamilies that exchange 1 Ca^{2+} (out) for 3 Na^+ (in) (11, 12). Three NCKX subfamilies have been found in vertebrates, exchanging 1 K^+ and 1 Ca^{2+} (out) for 4 Na^+ (in) (11). NCKX1 has been cloned from bovine (13), dolphin (14), chicken (15), rat (16), and human (17) retina rod cells. NCKX2 was originally identified in rat brain (18) and also retinal cone cells of chickens and humans (15). Both NCKX1 and -2 play crucial roles in regulating Ca^{2+} during phototransduction. Recently, a new subfamily, termed NCKX3, was discovered in rodents and humans (19). Unlike the restricted expression of NCKX1 and -2, NCKX3 is expressed in a variety of tissues, suggesting its widespread role in Ca^{2+} homeostasis. NCKX proteins are also involved in the *Drosophila* visual system (20), and have been found in the *Caenorhabditis elegans* genome (GenBank accession nos. NM_060203 and NM_073289).

Here we report a NCKX of animal spermatozoa. The sea urchin sperm NCKX (suNCKX) is a member of this family that localizes to the flagellar plasma membrane. In addition to showing K^+ and Na^+ dependence, an NCKX inhibitor blocks the exchanger's activity and sperm motility. The data support the hypothesis that the suNCKX maintains low intracellular Ca^{2+} , which is important for sperm motility before the sperm contacts the egg.

Materials and Methods

Cloning and Sequence Analysis. A suNCKX clone was isolated from a Lambda Zap II (Stratagene) cDNA library of *Strongylocentrotus purpuratus* testis. The full-length cDNA was made from three clones. suNCKX homologs were identified using BLAST searches (<http://www.ncbi.nlm.nih.gov/blast/>). Sites and motifs were identified using the ProfileScan web site (<http://hits.isb-sib.ch/cgi-bin/PFSCAN>). CLUSTALW (MacVector) was used for alignments. Transmembrane predictions used a window of 15 aa (21).

Phylogenetic Analysis. Complete sequences were used to construct a phylogenetic tree of NCKX proteins by the neighbor-joining method (22) with human NCX1 as an outgroup. The tree was validated by a bootstrap analysis with 1,000 replicates. GenBank accession numbers for NCKX sequences are: dolphin rod (dNCKX1), AF059031; bovine rod (bNCKX1), X66481; human rod (hNCKX1), AF062922; rat rod (rNCKX1), AF176688; chicken rod (cNCKX1), AF177984; chicken cone (cNCKX2), AF177985; rat brain (rNCKX2), AF021923; human cone (hNCKX2), AF097366; partial human (hNCKX3), AF169257; partial rat (rNCKX3), AY009158; partial mouse (mNCKX3), AF314821. Human (hNCX1) NM_021097 was used as an outgroup. The GenBank accession number of the suNCKX is AY077699.

Southern Blots. Ten micrograms of *Strongylocentrotus purpuratus* genomic DNA was digested and electrophoresed in 0.7% agarose and transferred to nylon membrane, which was probed with full-length suNCKX that was random-prime labeled with ^{32}P (DECAprime II, Ambion). Hybridization was at 65°C in 6 \times SSC (1 \times SSC = 0.15 M sodium chloride/0.015 M sodium citrate, pH 7)/5 \times Denhardt's/0.5% SDS/100 μ g/ml herring sperm DNA. The membrane was washed with 0.2 \times SSC/0.2% SDS at 65°C.

Northern Blots. Total RNA was isolated from sea urchin testis, eggs, and ovary with Trizol (Invitrogen). Twenty micrograms of

Abbreviations: ASW, artificial seawater; NaFSW, Na^+ -free artificial seawater; NCX, Na^+/Ca^{2+} exchanger; NCKX, K^+ -dependent Na^+/Ca^{2+} exchanger; TM, transmembrane segment; KB, KB-R7943 mesylate.

Data deposition: The sequence reported in this paper has been deposited in the GenBank database (accession no. AY077699).

*To whom reprint requests should be addressed. E-mail: vvacquier@ucsd.edu.

The publication costs of this article were defrayed in part by page charge payment. This article must therefore be hereby marked “advertisement” in accordance with 18 U.S.C. §1734 solely to indicate this fact.

RNA was separated on a formaldehyde agarose gel, transferred to nylon membrane, and hybridized with full-length ³²P-labeled suNCKX. Hybridization was at 60°C and washing was in 0.2× SSC/0.2% SDS.

Antibody Production. The peptide C-S⁷⁰DMQDKYQSDGN⁸¹, coupled to maleimide-activated KLH (Pierce), was used to make anti-P1 antibody in rabbits (Strategic BioSolutions). P1 antibody was purified on the peptide conjugated to Sulfo-Link resin (Pierce). Anti-EL antibody was made against suNCKX residues Leu⁶²–Leu¹¹² by expression using the pET system (Novagen). The protein was purified by Ni-NTA agarose (Qiagen) and coupled to BSA by using glutaraldehyde (23). Anti-EL antibody was affinity purified on EL-conjugated Affigel-10 (Bio-Rad).

Western Blots. Sea urchins were spawned by injection of 0.5 M KCl and undiluted sperm collected and stored on ice <12 h before use. Sperm membrane vesicles were isolated (24), and the proteins separated on SDS/PAGE and transferred to nitrocellulose. The membrane was probed with anti-P1 or anti-EL antibody, detected with an HRP-conjugated goat anti-rabbit secondary antibody, and developed with SuperSignal West Dura Extended Duration Substrate (Pierce).

Immunolocalization. Sperm were fixed in seawater with 3% paraformaldehyde and 0.1% glutaraldehyde. Fixed cells were blocked in 150 mM NaCl/10 mM Hepes (pH 7.8)/5% normal goat serum (Sigma). Samples were incubated with anti-P1 or anti-EL antibody and detected with Alexafluor 546 goat anti-rabbit IgG (Molecular Probes).

Measurement of Intracellular Ca²⁺. Undiluted sperm (stored <12 h) were diluted 50-fold and washed twice in Na⁺-free seawater (NaFSW: 486 mM choline chloride/10 mM CaCl₂/7.5 mM KCl/27 mM MgCl₂/29 mM MgSO₄/2.5 mM KHCO₃/10 mM Hepes, adjusted to pH 7.9 with 1 M *N*-methyl-D-glucamine) for Na⁺-dependency experiments, or K⁺/divalent cation-free seawater (KDFSW: 480 mM NaCl/10 mM Hepes, adjusted to pH 8 with NaOH) for K⁺-dependency experiments. The same buffers containing 12 μM fura-2AM (Molecular Probes) were used during dye loading. The solid fura-2AM was dissolved in anhydrous DMSO at 2 mM. Based on the starting volume of undiluted sperm, the cells were diluted 5-fold during loading. All procedures for loading sperm cells were done on ice in the dark for at least 8 h. Free fura-2 was removed by centrifugation at 1,000 × *g* for 10 min at 4°C. Cell pellets were washed twice in the same buffer without fura-2. The final cell pellets were resuspended in 5 vol fresh buffer and stored on ice in the dark. For Ca²⁺ measurements, 50 μl of fura-2-loaded sperm (2 × 10⁸ cells per ml) were diluted in 1.5 ml of 10 mM Hepes (pH 7.8)-buffered medium containing different salts, as described in the figure legends. Ca²⁺ measurements were at 16°C under constant stirring in a FluoroMax-2 fluorometer with excitation at 340 and 380 nm, and emission at 500 nm. The ratio of emission intensities with 340 and 380 nm excitation (F340/F380) reports relative intracellular [Ca²⁺]. In this paper, [Ca²⁺]_i is expressed either as F340/F380 or calibrated into [Ca²⁺]_i/K_d (25).

Sperm Motility. Sperm were diluted into 0.5% (wt/vol) polyvinylpyrrolidone (40,000 molecular weight) in artificial seawater (ASW: 486 mM NaCl/10 mM CaCl₂/10 mM KCl/27 mM MgCl₂/29 mM MgSO₄/2.5 mM NaHCO₃/10 mM Hepes, adjusted to pH 7.9 with 1 M NaOH). Sperm motility was observed using dark field conditions. Sperm were photographed (1-s exposure) 1 min after mixing with various concentrations of the NCKX inhibitor, KB-R7943 mesylate (Tocris Cookson, Ellisville, MO). The inhibitor was dissolved in DMSO to 50 mM and then diluted into the test solution of 1.5 ml.

Results

Sequence and Phylogenetic Analysis. Full-length suNCKX has two 5'ATG codons downstream of an in-frame stop codon. We assigned the second ATG as the initiation codon because it conforms best to the Kozak (26) consensus sequence for translation initiation, AcaATGC (uppercase indicates matches with suNCKX). The ORF is 1,956-bp and encodes a protein of 652 aa with a calculated molecular mass of ≈72 kDa, showing relatedness to human, rat, and chicken NCKX sequences (Fig. 1A). The hydropathy analysis (Fig. 1B) suggests 12 transmembrane segments (TM) similar to other NCKX proteins (Fig. 1A–C). Like other NCKXs, the predicted suNCKX (Fig. 1C) begins with a cytoplasmic NH₂ terminus, transmembrane segment 1 (TM1), an extracellular loop of 46 residues, a cluster of five transmembrane segments (TM2–TM6), a cytoplasmic loop of 183 residues, and a hydrophobic cluster (TM7–TM12) with a short cytoplasmic COOH terminus. suNCKX contains five potential N-linked glycosylation sites (Fig. 1A, arrows), two being putatively extracellular, one of which is in the external loop between TM1 and -2, and the other between TM7 and -8. There are two protein kinase A (PKA) sites in the cytoplasmic loop between TM6 and -7 (asterisks). suNCKX also contains an unusual His-rich region from His-352 to His-395 in its intracellular loop, where 15 of 44 residues are His, with seven His residues being contiguous.

The multiple sequence alignment (Fig. 1A) shows that the most conserved regions among different NCKXs are the 12 TM, and especially the two α-repeat regions, containing TM3–TM4 and TM9–TM10, which are thought to represent the ion binding sites (27). Outside these regions, for example in the cytoplasmic loop, the similarities among NCKXs decrease. However, the potential N-linked glycosylation site in the extracellular loop is conserved among the four NCKXs (Fig. 1A). One unusual finding is that only one Cys residue (TM2) is conserved in all four sequences. The overall amino acid identity between suNCKX and vertebrate NCKXs is 25 to ≈28% (similarity = 42 to ≈44%). Within the two α-repeat regions, suNCKX and other NCKXs are 64 to ≈72% identical and 81 to ≈83% similar. The highest conservation among NCKXs is in TM3, where 20 of 25 positions are identical.

A phylogenetic tree based on full-length NCKX proteins (Fig. 2) shows that suNCKX does not group with the three vertebrate subfamilies, but branches at the base of the vertebrate lineage. This analysis reveals a division of vertebrate NCKX proteins into NCKX3 on one hand, and NCKX1 plus NCKX2 on the other. NCKX1 and NCKX2 are specifically expressed in rod and cone cells and neurons, suggesting a conserved function in photo-transduction. In contrast to the restricted expression of NCKX1 and NCKX2, the newly discovered NCKX3 subfamily is expressed in various tissues, suggesting a widespread role in Ca²⁺ regulation (19).

suNCKX Is a Single Gene. Southern blot analysis was performed to determine the copy number of suNCKX in the sea urchin genome (Fig. 3A). Restriction enzymes *Nde*I (N), *Swa*I (S), *Xba*I (Xb), and *Xho*I (Xh), with no cutting site within the ORF, yielded one band of hybridization as detected using a full-length probe. *Eco*RV (E), with one recognition site within the ORF, yielded two bands of hybridization. These data show that suNCKX is encoded by a single copy gene.

suNCKX Expression. To determine suNCKX expression, total RNA was isolated from egg, ovary, and testis, electrophoresed, blotted onto membrane, and hybridized to a full-length ³²P-labeled suNCKX (Fig. 3B). The result shows that suNCKX is predominantly expressed in testis, although the same bands appeared in egg and ovary samples after longer exposures (data not shown). In addition to the major 4.4-kb band in testis RNA,

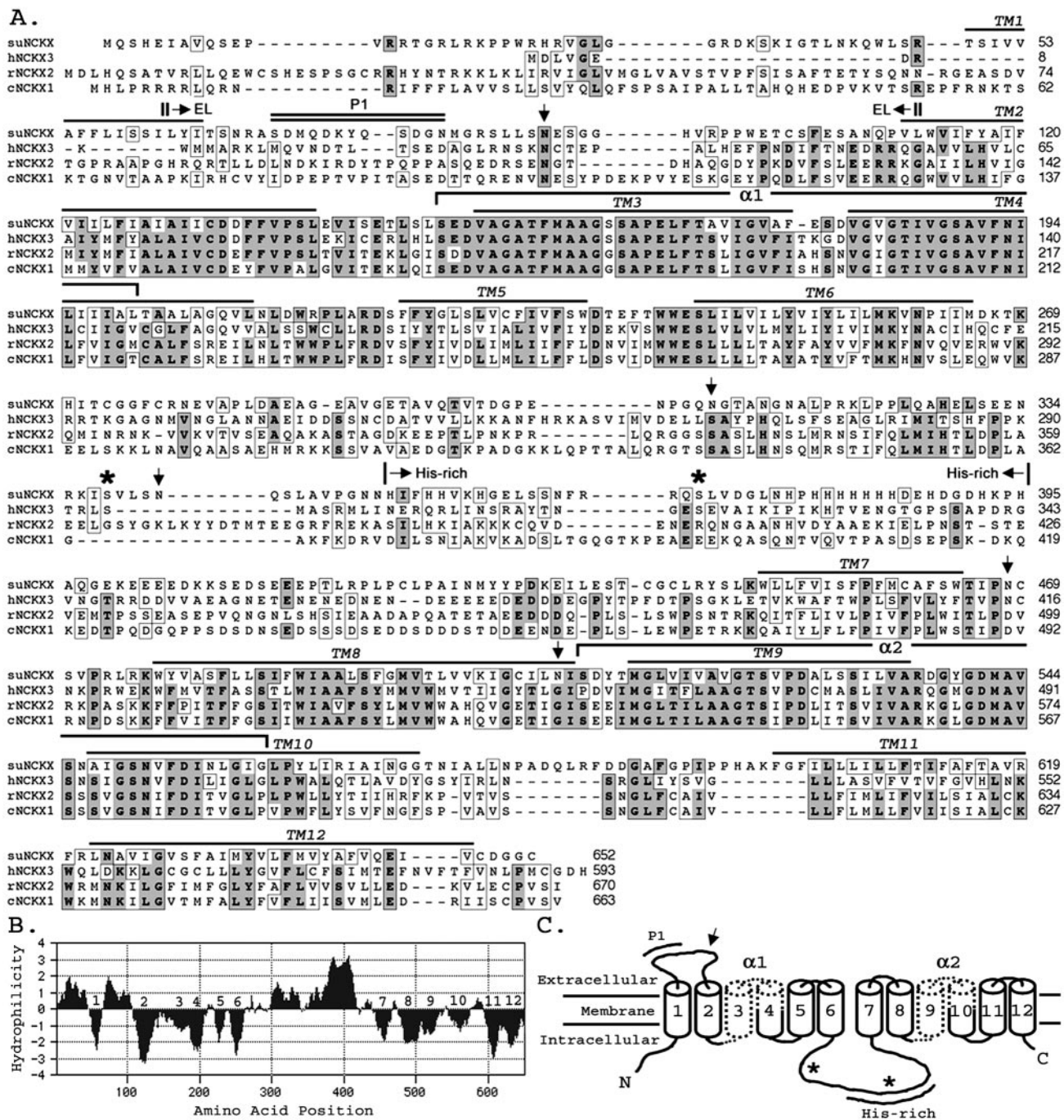


Fig. 1. Sequence and topology of suNCKX. (A) Amino acid alignment of suNCKX, human (hNCKX3), rat (rNCKX2), and chicken (cNCKX1). Residues identical in three or four sequences are shown in boldface type and dark shading. Similar residues are boxed. Amino acid positions are on right. Locations of putative transmembrane segments (TM1–12) are overlined. Two α repeats are shown as brackets. Downward arrows show five putative N-linked glycosylation sites, and asterisks indicate the two putative protein kinase A sites. The His-rich region is denoted by arrows above the sequence. Antigens used to produce antibodies are indicated as P1 (double overline) and EL (\rightarrow). (B) Hydropathy plot of suNCKX. numbers (1–12) denote the putative transmembrane segments. (C) Schematic model of suNCKX: 12 transmembrane segments (cylinders), two α repeats (dotted), one conserved N-linked glycosylation site (\downarrow), two protein kinase A sites (*), His-rich region, and the location of P1 peptide are indicated. GenBank accession no. AY077699.

there is also a band of larger size that could represent partially processed suNCKX mRNA.

suNCKX Is an \approx 90-kDa Flagellar Protein. Sperm membrane proteins were separated by SDS/PAGE and transferred to nitrocellulose membrane, and immunoblots were performed with anti-P1 or anti-EL antibody. Both anti-P1 and anti-EL react with a single

band at \approx 90 kDa (Fig. 4A and data not shown), which is larger than the calculated molecular mass of \approx 72 kDa. Although suNCKX has five potential N-linked glycosylation sites, the mobility of the band was unaltered after protein N-glycosidase F treatment of the sample (data not shown). Silver-stained gels show the \approx 90-kDa protein is not a major component of total sperm membrane proteins, although suNCKX is heavily ex-

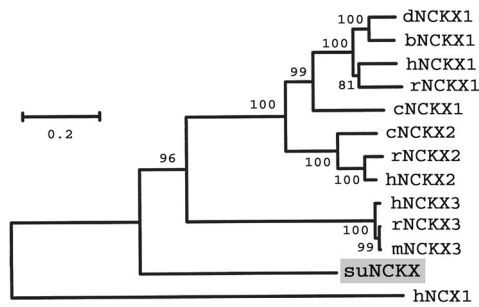


Fig. 2. Phylogenetic tree of NCKX proteins. The tree was constructed by neighbor joining with human NCX1 as the outgroup. Values at branch points are bootstrap percentages with 1,000 replications. GenBank accession numbers are in *Material and Methods*. d, dolphin; b, bovine; h, human; r, rat; c, chicken; m, mouse. The suNCKX branches before the split giving rise to the three types of vertebrate NCKXs. The scale indicates % amino acid difference with the Poisson correction.

pressed in the testis. Immunofluorescence localization on whole sperm, using anti-P1 antibody, shows that suNCKX is localized over the entire sperm flagellum and the mitochondrion, but not the sperm head (Fig. 4B).

NCKX Activity. Fura-2-loaded sperm in NaFSW were used to test the dependency of Ca^{2+} efflux on the addition of Na^+ . Sperm in NaFSW have higher internal Ca^{2+} because the suNCKX cannot function without external Na^+ . Sperm were suspended in NaFSW and the fluorescence recorded for 2 min before the addition of an equal volume of 486 mM Na^+ containing ASW. An immediate decrease in sperm Ca^{2+} occurred that was sustained until the end of the recording (Fig. 5A). Addition of an equal volume of NaFSW did not induce Ca^{2+} efflux. The small increase in sperm Ca^{2+} in the NaFSW trace is due to the dilution of the fura-2-loaded cells.

To test the K^+ dependency of Ca^{2+} influx, the exchanger was made to run in reverse mode as previously demonstrated for other NCKXs (14–16, 18, 19). Sperm were loaded with fura-2 in buffer lacking K^+ and divalent cations [KDFSW (K^+ and divalent cation free artificial seawater)], which raises intracellular Na^+ . The 50- μl sample of sperm in 480 mM Na^+ -containing buffer was diluted into 1.5 ml of 480 mM Li^+ -containing buffer, with or without 10 mM K^+ . If the suNCKX activity is present in sea urchin sperm this will reverse the Na^+ gradient and favor Ca^{2+} entry into the cells in the presence of extracellular K^+ . As shown in Fig. 5B, the cells showed a greater Ca^{2+} increase in the Li^+ + K^+ solution than they did to cells in

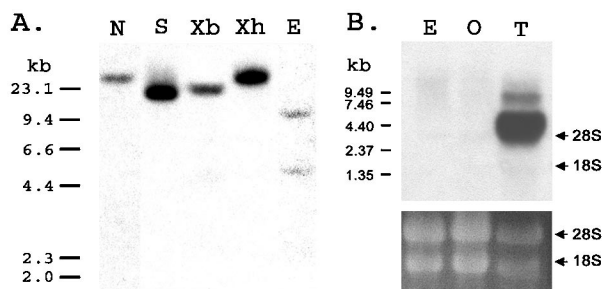


Fig. 3. (A) Southern blot analysis of suNCKX. Each lane had 10 μg of genomic DNA that was digested with *Nde*I (N), *Swa*I (S), *Xba*I (Xb), *Xho*I (Xh), and *Eco*RV (E). Size markers are on the left in kb. (B) Northern blot. Twenty micrograms of total RNA was isolated from egg (E), ovary (O), and testis (T) and analyzed by Northern blotting at high stringency, using a full-length suNCKX as a probe. Size markers are at left, and the positions of 18S and 28S rRNA are indicated at right. (Bottom) Equivalent rRNA bands in each lane as a control for loading.

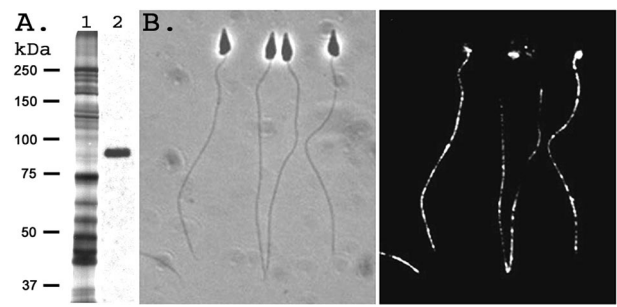


Fig. 4. Immunoblot and immunolocalization with suNCKX antibody. (A) Lane 1 is a silver stained gel of total sperm membrane vesicle protein; lane 2 is the same sample reacted with anti-P1 antibody. Relative molecular masses are on left; 2.5 μg protein on lane 1, and 5 μg on lane 2. (B) Immunolocalization of suNCKX with anti-P1 antibody. (Left) Phase contrast image; (Right) immunofluorescence. The width of each sperm head is $\approx 1 \mu\text{m}$.

the Li^+ solution, showing that suNCKX is K^+ -dependent and can run in reverse mode. In summary, the above experiments show that suNCKX activity depends on both Na^+ and K^+ for Ca^{2+} transport.

KB-R7943 Mesylate Inhibits suNCKX. KB-R7943 mesylate (KB) was originally identified as a NCX inhibitor (28). However, a recent study showed that it also inhibits NCKX (29). We found that KB at 10 and 20 μM caused an immediate Ca^{2+} influx in fura-2-loaded sperm in ASW (Fig. 6A). A final concentration of 50 μM KB was required to completely inhibit Na^+ -dependent Ca^{2+} efflux (Fig. 6B). However, only 10 μM was required to block K^+ -dependent Ca^{2+} influx (Fig. 6C). Greater sensitivity to KB in the reverse mode is consistent with results with other NCX and NCKX exchangers (28, 30). The compound CGP37157, a specific blocker of mitochondrial NCX (31), and the Ca^{2+} channel blockers nifedipine, verapamil, and Ni^{2+} (10) had no effect on both Na^+ -dependent Ca^{2+} efflux and K^+ -dependent Ca^{2+} influx. These negative results were also obtained in 20 μM oligomycin, showing that mitochondrial ion flux and ATP are not involved in the Na^+ -mediated Ca^{2+} efflux (data not shown). These data indicate that the Na^+ -dependent Ca^{2+} efflux, and reverse mode K^+ -dependent Ca^{2+} influx, measured in our experiments are not mediated by NCX or Ca^{2+} channels. The inhibition of Ca^{2+} transport by KB (but not CGP37157) further confirms that suNCKX activity is present in sea urchin sperm.

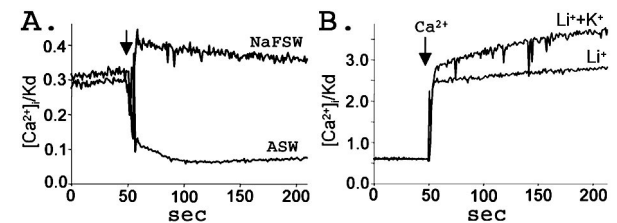


Fig. 5. NCKX activities in sea urchin sperm. (A) Na^+ -dependent Ca^{2+} efflux. Sperm were loaded with fura-2 in NaFSW. For measurements, 50 μl fura-2-loaded sperm were diluted into 1.5 ml of NaFSW, and after 2 min an equal volume of NaFSW or ASW was added as indicated by the arrow. Rapid efflux of Ca^{2+} occurred in ASW. (B) K^+ -dependent Ca^{2+} influx. Sperm were loaded with fura-2 in K^+ and divalent cation free artificial seawater (KDFSW) and diluted into Li^+ / K^+ solution (480 mM LiCl /10 mM KCl /1 mM EGTA/20 mM HEPES, adjusted to pH 8 with 1 M *N*-methyl-D-glucamine), or Li^+ solution (490 mM LiCl /1 mM EGTA/20 mM HEPES, pH 8 with *N*-methyl-D-glucamine) as indicated. Ten micromolar CaCl_2 was added at the arrow. More Ca^{2+} entered the cells in the 10 mM K^+ sample, showing that suNCKX can run in reverse mode. Data are from a representative experiment repeated seven times.

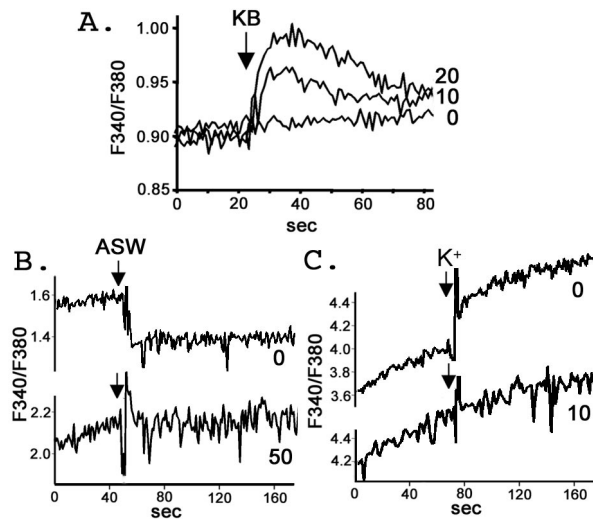


Fig. 6. KB-R7943 mesylate blocks suNCKX activity. (A) KB causes Ca^{2+} influx. KB was added to fura-2-loaded sperm in ASW at the arrow. The final concentration of KB in μM is shown on the right. (B) KB blocks Na^{+} -dependent Ca^{2+} efflux. Fura-2-loaded sperm were prepared as in Fig. 5A. Sperm were mixed with various concentrations of KB (final μM shown on right) 2 min before addition of an equal volume of ASW at the arrow. (C) KB blocks K^{+} -dependent Ca^{2+} influx. Fura-2-loaded sperm were diluted into Li^{+} solution plus 10 mM CaCl_2 with various concentrations of KB (μM final on right) 2 min before the addition of 10 mM KCl at the arrow. Experiments were repeated three times.

The Ca^{2+} influx by KB in ASW suggests the function of suNCKX in sea urchin sperm is to keep Ca^{2+} low.

KB is a potent inhibitor of sperm motility in normal seawater (Fig. 7). One micromolar KB partially blocks sperm motility (Fig. 7C), and 4 μM inhibits sperm motility completely within 1 min (Fig. 7E). Again, CGP37157 has no effect on sperm motility at the same concentration as KB (data not shown). As shown in Fig. 6A, the increase in cytosolic Ca^{2+} occurred on the same time scale as the onset of immotility. The low concentration and rapid inhibition by KB suggests that sperm motility is sensitive to the level of intracellular Ca^{2+} and that suNCKX activity is crucial for Ca^{2+} -regulated motility (2–9). Inhibition of motility by KB was not due to general cytotoxicity; ciliated sea urchin gastrulae swam normally and continued normal development after 24 h in 20 μM KB.

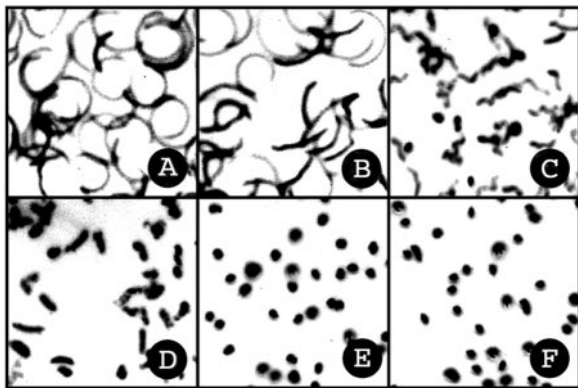


Fig. 7. KB-R7943 mesylate inhibits sperm motility. Photographs were taken 1 min after sperm were mixed with KB. The final concentrations of KB in μM are: A, 0; B, 0.5; C, 1; D, 2; E, 4; and F, 8. Each track is the dark field image of the refractile sperm head path during the 1-s exposure. In A, individual sperm cells are fully motile and scribe circular paths. In E, sperm are immotile and individual sperm heads are seen as dots.

Discussion

Ion channels regulate the metabolism, swimming, and induction of the acrosome reaction of sea urchin sperm (10). To our knowledge, no ion exchangers have until now been cloned from these cells. Here we report the sequence of an NCKX from animal sperm and suggest that it is involved in maintaining the low intracellular Ca^{2+} concentrations necessary for sperm motility. Although we did not exogenously express suNCKX and determine its stoichiometry of exchange, that it is a new NCKX family member, typical of other homologs, is supported by the following data: the sequence similarity and high percent identity in the 12 TM segments and the two α repeats; the topology of TMs similar to other NCKX proteins with the extracellular loop between TM1–2 with a conserved N-linked glycosylation site; the large cytoplasmic loop between TM6–7, also typical of other NCKX homologs (Fig. 1); closer similarity to NCKX than to NCX proteins (Fig. 2); dependence on extracellular Na^{+} for Ca^{2+} efflux; K^{+} dependence in reverse mode for Ca^{2+} influx; localization over the flagellum; and inhibition of NCKX-mediated exchange and sperm motility by KB-R7943 mesylate. The activity of suNCKX might explain why it is impossible to load sea urchin sperm with $^{45}\text{Ca}^{2+}$, regardless of the external Ca^{2+} concentration (V.D.V., unpublished data). However, in NaFSW the fura-2-loaded cells do take up Ca^{2+} as shown by higher F340/F380 than those observed in seawater (Fig. 6A and B).

Although we document the existence of suNCKX activity in animal sperm, we have not excluded the possibility that NCX activity also exists in these cells. NCX activity was reported in plasma membrane vesicles from ram sperm flagella, the activity having characteristics similar to NCX of heart, brain, and squid axons. An interesting characteristic of ram sperm NCX is its inhibition by the Ca^{2+} channel blocker verapamil (32). A bovine sperm plasma membrane vesicle NCX activity was higher in epididymal sperm than in ejaculated sperm. This NCX runs in reverse mode, bringing Ca^{2+} into cells in an ATP-independent, Na^{+} -dependent manner. During ejaculation, a seminal plasma inhibitor binds to the NCX to lower its activity (33). Herring sperm are immotile when spawned, but motility initiates when they bind a factor released from eggs. Motility initiation depends on an NCX that brings Ca^{2+} into the sperm in exchange for Na^{+} efflux (34).

Vertebrates have several NCKX genes coding for tissue-specific forms of the protein. Fig. 2 shows their evolution by two gene duplications giving rise to the three subfamilies of vertebrate NCKX proteins. However, sea urchins appear to have only one NCKX gene (Fig. 3A), which is highly, but not exclusively, expressed in testes (Fig. 3B). Sea urchins are echinoderms, the lowest deuterostome animals (the branch leading to the vertebrates). Between echinoderms and humans, several rounds of genome duplication have occurred, as shown by the sea urchin genome size of 800 megabases (Mb) versus 3,200 Mb for humans. Sea urchins also have one cluster of Hox genes, whereas mammals have four (35). Study of suNCKX in embryos and adults will be of interest for understanding suNCKX physiology in lower deuterostomes. All flagellated and ciliated cells living in seawater have the same problem of keeping internal Ca^{2+} low. The general finding with marine cells is that, internally relative to externally, they are high in K^{+} and low in Na^{+} , thus being ideal for supporting high NCKX activity. NCKX proteins could be widely distributed in single-celled marine organisms.

NCKX proteins exist in two forms: of approximately 650 and 1,200 residues. Most of the difference in length involves the putative cytoplasmic loop. Expression of chimeric NCKX proteins shows that the NH_2 -terminal part of the loop binds Ca^{2+} and confers K^{+} dependency on ion exchange (36). The suNCKX is 652 residues with a relatively short cytoplasmic loop of 183

residues. Of interest within the loop are the two protein kinase A (PKA) sites and the His-rich region. When sea urchin sperm swim into the egg jelly layer, large transient increases in guanylyl cyclase and adenylyl cyclase activities occur, in addition to the influx of Ca^{2+} and Na^+ and the efflux of K^+ and H^+ (10, 37). Egg jelly induces a ≈ 50 -fold activation of PKA (37), which could phosphorylate these two suNCKX sites and alter the structure and charge of the loop, influencing the binding of metal ions in the His-rich domain. A transient reversal of the suNCKX activity could explain the influx in Ca^{2+} on treatment of sperm with the egg peptide speract (37–39).

In the His-rich region of the cytoplasmic loop, which is unique to suNCKX, 15 of 44 residues are His. Histidine is the only amino acid with a pK of 6.0, the closest pK to sperm pH of 7.2 (40). At pH 6.0 more than half of the His residues would be positively charged, but at pH 7.0 less than 10% would be positively charged. Sperm motility is extremely sensitive to intracellular pH, because axonemal dynein has a very steep pH-dependency curve (41). Sperm pH is known to be controlled by the activity of an Na^+/H^+ exchanger that is activated when sperm are spawned into seawater, resulting in an increase in cellular pH from 7.2 to 7.6 (40, 42). The phosphorylation–dephosphorylation of the PKA sites and intracellular pH changes could regulate metal ion binding to the 15 His residues, and alter the helical content of the cytoplasmic loop, which could in turn modulate the activity of the suNCKX to keep Ca^{2+} levels constantly low for optimal swimming.

In rod cells, NCKX is physically bound to the α -subunit of a cGMP-gated cation channel (43). Sea urchin sperm have high

levels of membrane bound guanylyl cyclase that is activated by the egg peptide speract (10, 37). cGMP in turn regulates a K^+ channel that hyperpolarizes the sperm membrane (10, 44, 45). The suNCKX activity could also be physically associated with the sperm cGMP-regulated channel and guanylyl cyclase, all of which are localized in the sperm flagellar membrane. These proteins could form a complex for tight physiological control of membrane potential, intracellular pH, and intracellular Ca^{2+} . A cAMP-modulated, weakly selective cation channel, termed I_{h} , has been cloned from sea urchin sperm that localizes to the flagellar plasma membrane (46). Sperm specific ion channels also regulate cation flux in mammalian sperm flagella, although the mechanism of regulation remains unknown at this time (47–49).

When swimming sea urchin sperm contact egg jelly, two Ca^{2+} channels sequentially activate that elevate Ca^{2+} to induce the sperm acrosome reaction, an exocytosis necessary for sperm–egg fusion (10). After the acrosome reaction, Ca^{2+} enters the cell and is sequestered in the mitochondrion (38). The suNCKX is either inactivated on contact with the egg jelly, or merely overwhelmed by the rapid, massive influx of Ca^{2+} , allowing the Ca^{2+} concentration to rise to levels permissive for acrosome reaction induction. Further study of the suNCKX will aid in our understanding of the regulation of the control of ion flux across the sperm membrane.

Dr. Charles G. Glabe is thanked for peptide P1. This work was supported by National Institutes of Health Grant HD12986.

1. Bootman, M. D. & Berridge, M. J. (1995) *Cell* **83**, 675–678.
2. Sale, W. S. (1986) *J. Cell Biol.* **102**, 2042–2052.
3. Ishijima, S. & Hamaguchi, Y. (1993) *Biophys. J.* **65**, 1445–1448.
4. Bannai, H., Yoshimura, M., Takahashi, K. & Shingyoji, C. (2000) *J. Cell Sci.* **113**, 831–839.
5. Brokaw, C. J., Josslin, R. & Bobrow, L. (1974) *Biochem. Biophys. Res. Commun.* **58**, 795–800.
6. Brokaw, C. J. (1979) *J. Cell Biol.* **82**, 401–411.
7. Gibbons, B. H. & Gibbons, I. R. (1980) *J. Cell Biol.* **84**, 13–27.
8. Brokaw, C. J. (1991) *Cell Motil. Cytoskel.* **18**, 123–130.
9. Gibbons, B. H. (1980) *J. Cell Biol.* **84**, 1–12.
10. Darszon, A., Beltran, C., Felix, R., Nishigaki, T. & Trevino, C. L. (2001) *Dev. Biol.* **240**, 1–14.
11. Blaustein, M. P. & Lederer, W. J. (1999) *Physiol. Rev.* **79**, 763–854.
12. Philipson, K. D. & Nicoll, D. A. (2000) *Annu. Rev. Physiol.* **62**, 111–133.
13. Reilander, H., Achilles, A., Friedel, U., Maul, G., Lottspeich, F. & Cook, N. J. (1992) *EMBO J.* **11**, 1689–1695.
14. Cooper, C. B., Winkfein, R. J., Szerencsei, R. T. & Schnetkamp, P. P. M. (1999) *Biochemistry* **38**, 6276–6283.
15. Prinsen, C. F. M., Szerencsei, R. T. & Schnetkamp, P. P. M. (2000) *J. Neurosci.* **20**, 1424–1434.
16. Poon, S., Leach, S., Li, X. F., Tucker, J. E., Schnetkamp, P. P. M. & Lytton, J. (2000) *Am. J. Physiol. Cell Physiol.* **278**, C651–C660.
17. Tucker, J. E., Winkfein, R. J., Cooper, C. B. & Schnetkamp, P. P. M. (1998) *Invest. Ophthalmol. Vis. Sci.* **39**, 435–440.
18. Tsoi, M., Rhee, K. H., Bungard, D., Li, X. F., Lee, S. L., Auer, R. N. & Lytton, J. (1998) *J. Biol. Chem.* **273**, 4155–4162.
19. Kraev, A., Quednau, B. D., Leach, S., Li, X. F., Dong, H., Winkfein, R., Perizzolo, M., Cai, X., Yang, R., Philipson, K. D. & Lytton, J. (2001) *J. Biol. Chem.* **276**, 23161–23172.
20. Haug-Collet, K., Pearson, B., Webel, R., Szerencsei, R. T., Winkfein, R. J., Schnetkamp, P. P. M. & Colley, N. J. (1999) *J. Cell Biol.* **147**, 659–669.
21. Kyte, J. & Doolittle, R. F. (1982) *J. Mol. Biol.* **157**, 105–132.
22. Kumar, S., Tamura, K., Jakobsen, I. B. & Nei, M. (2001) MEGA2: Molecular Evolutionary Genetics Analysis Software (Arizona State Univ., Tempe, AZ), Version 2.
23. Carter, J. M. (1996) in *The Protein Protocols Handbook*, ed. Walker, J. M. (Humana, Totowa, NJ), pp. 679–687.
24. Podell, S. B., Moy, G. W. & Vacquier, V. D. (1984) *Biochim. Biophys. Acta* **778**, 25–37.
25. Kao, J. P. Y. (1994) *Methods Cell Biol.* **40**, 155–181.
26. Kozak, M. (1996) *Mamm. Genome* **7**, 563–574.
27. Schwarz, E. M. & Benzer, S. (1997) *Proc. Natl. Acad. Sci. USA* **94**, 10249–10254.
28. Iwamoto, T., Watano, T. & Shigekawa, M. (1996) *J. Biol. Chem.* **271**, 22391–22397.
29. Takano, S., Kimura, J. & Ono, T. (2001) *Br. J. Pharmacol.* **132**, 1383–1388.
30. Nakamura, H., Kawasaki, Y., Arakawa, N., Saeki, M., Maeda, S., Koyama, Y., Baba, A. & Matsuda, T. (2000) *Neurochem. Res.* **25**, 385–387.
31. Cox, D. A., Conforti, L., Sperelakis, N. & Matlib, M. A. (1993) *J. Cardiovasc. Pharmacol.* **21**, 595–599.
32. Bradley, M. P. & Forrester, I. T. (1980) *FEBS Lett.* **121**, 15–18.
33. Rufo, G. A., Jr., Schoff, P. K. & Lardy, H. A. (1984) *J. Biol. Chem.* **259**, 2547–2552.
34. Vines, C. A., Yoshida, K., Griffin, F. J., Pillai, M. C., Morisawa, M., Yanagimachi, R. & Cherr, G. N. (2002) *Proc. Natl. Acad. Sci. USA* **99**, 2026–2031.
35. Martinez, P., Lee, J. C. & Davidson, E. H. (1997) *J. Mol. Evol.* **44**, 371–377.
36. Seiler, E. P., Guerini, D., Guidi, F. & Carafoli, E. (2000) *Eur. J. Biochem.* **267**, 2461–2472.
37. Garbers, D. L. (1989) *Annu. Rev. Biochem.* **58**, 719–742.
38. Schackmann, R. W. & Chock, P. B. (1986) *J. Biol. Chem.* **261**, 8719–8728.
39. Cook, S. P., Brokaw, C. J., Muller, C. H. & Babcock, D. F. (1994) *Dev. Biol.* **165**, 10–19.
40. Johnson, C. H., Clapper, D. L., Winkler, M. M., Lee, H. C. & Epel, D. (1983) *Dev. Biol.* **98**, 493–501.
41. Christen, R., Schackmann, R. W. & Shapiro, B. M. (1983) *J. Biol. Chem.* **258**, 5392–5399.
42. Lee, H. C. (1985) *J. Biol. Chem.* **260**, 10794–10799.
43. Schwarzer, A., Schauf, H. & Bauer, P. J. (2000) *J. Biol. Chem.* **275**, 13448–13454.
44. Cook, S. P. & Babcock, D. F. (1993) *J. Biol. Chem.* **268**, 22402–22407.
45. Galindo, B. E., Beltran, C., Cragoe, E. J., Jr., & Darszon, A. (2000) *Dev. Biol.* **221**, 285–294.
46. Gauss, R., Seifert, R. & Kaupp, U. B. (1998) *Nature (London)* **393**, 583–587.
47. Ren, D., Navarro, B., Perez, G., Jackson, A. C., Hsu, S., Shi, Q., Tilly, J. L. & Clapham, D. E. (2001) *Nature (London)* **413**, 603–609.
48. Quill, T. A., Ren, D., Clapham, D. E. & Garbers, D. L. (2001) *Proc. Natl. Acad. Sci. USA* **98**, 12527–12531.
49. Garbers, D. L. (2001) *Nature (London)* **413**, 579–582.